Evenstar, L. A., Stuart, F., Hartley, A., & Tattitch, B. C. (2015). Slow Cenozoic uplift of the western Andean Cordillera indicated by cosmogenic ^{3}He in alluvial boulders from the Pacific Planation Surface: Slow Cenozoic uplift of the Andes . *Geophysical Research Letters*, *42*(20), 8448-8455. https://doi.org/10.1002/2015GL065959

Slow Cenozoic uplift of the western Andean Cordillera indicated by cosmogenic ^{3}He in alluvial boulders from the Pacific Planation Surface.

Laura A. Evenstar

School of Earth Science, University of Bristol, Wills Memorial Building, Queens Road, Bristol, BS8 1RJ, UK (l.evenstar@bristol.ac.uk)

Finlay M. Stuart

Isotope Geoscience Unit, Scottish Universities Environmental Research Centre, East Kilbride, G75 0QF, UK

Adrian J. Hartley,

Dept. of Geology and Petroleum Geology, University of Aberdeen, Aberdeen, AB24 3UE, UK

Brain Tattitch

School of Earth Science, University of Bristol, Wills Memorial Building, Queens Road, Bristol, BS8 1RJ, UK

Key Points;

- Production rates of *in situ* cosmogenic isotopes are used for paleoelevation.
- Uplift of the Andes by mantle delamination in the Late Miocene is ruled out.
- The Precordillera attained a substantial part of its elevation by 14 Ma.

Running title; Slow Cenozoic uplift of the Andes

Abstract

To determine the mechanisms responsible for mountain belt growth it is important to accurately establish the timing of surface uplift. Here we exploit the altitude control on the production rate of *in situ* cosmogenic nuclides to test the hypothesis that the Andes were uplifted in the late Miocene. High concentrations of *in situ* cosmogenic ^{3}He ($^{3}He_{cos}$) have previously been measured in alluvial boulders on the western flank of the Central Andes, northern Chile (Evenstar et al. 2009). These are consistent with deposition soon after formation of the surface (13-14 Ma). We have modelled the accumulation of cosmogenic ^{3}He in several different surface uplift scenarios and compared them to the measured concentrations. The measured $^{3}He_{cos}$ concentrations are too high to be produced by late Miocene uplift and imply that the western flank of the Andean Cordillera attained a substantial part of its current elevation prior to 14 million years ago.

Number of words; 149

Keywords: *Andean Uplift; Cosmogenic Isotopes; Paleoelevation; Longitudinal Valley, Chile*

1. Introduction

The elevation history of mountain belts such as the Himalayas, North American Rockies, Andes and Alps have been used to explain continental tectonic processes, orogenic erosion and changes to the global climate (e.g. Clift, 2010). However there is typically a significant uncertainty associated with the timing and magnitude of surface uplift that has led to a wide range of mechanisms to account for orogenic uplift.

The lack of unequivocal constraints on the mean elevation history of the Central Andes has lead to competing theories to account for the generation of the mountain belt. These hypotheses have been simplified into two general scenarios by Barnes and Ehler (2009): (i) Late Miocene uplift, where surface uplift of ~2.5 km occurred between 11 and 6 Ma (Farías et al. 2005; Garzione et al. 2006; Ghosh et al. 2006; Molnar and Garzione 2007; Garzione et al. 2008; Hoke and Garzione 2008) due to large-scale mantle delamination, and (ii) Early Miocene (or earlier) uplift, where gradual surface uplift initiated in the Late Eocene is associated with crustal shortening and thickening in response to oblique subduction of the Nazca plate (e.g. Victor et al. 2004; Barke and Lamb 2006; Hartley et al. 2007; Barnes and Ehlers 2009).

The evidence for Late Miocene uplift is based on a number of studies that have utilised climate-sensitive altitude relationships, such as oxygen isotopes (Garzione et al. 2006), clumped C-O isotopes (Ghosh et al. 2006; Quade et al. 2007) and fluvial incision rate (Schildgen et al. 2007; Hoke et al. 2007; Thouret et al. 2007). The isotope-based techniques assume that the present-day relationship between meteoritic water, surface temperatures and elevation can be used to reconstruct past elevations suggest the majority of uplift occurred after 10 Ma. However there are a number of uncertainties associated with this technique (Hartley et al. 2007, Ehler and Poulsen 2009; Jeffery et al. 2013). Recent modelling of climate change associated with Andean uplift shows that this overestimates uplift rates, as precipitation levels, surface temperature and wind direction have varied during uplift (Ehler and Poulsen 2009). It also predicts an increase in precipitation along the Western Cordillera that would account for the rapid fluvial incision, rather than resulting from surface uplift (Jeffery et al. 2013). A recent re-assessment suggests that the existing data cannot distinguish between Late Miocene or Early Miocene (or earlier) uplift histories leading to an array of competing theories to account for the generation of the mountain belt (Barnes and Ehler 2009). Without independent constraints on the timing and rate of surface

uplift it is difficult to determine which tectonic processes are responsible for the formation of the Andean mountain belt.

The production rate of *in situ* cosmogenic nuclides at the Earth surface is strongly altitude dependent and where slowly eroding surfaces are preserved they have the potential to be used to decipher the surface uplift history of mountain ranges that is independent of climate (e.g. Riihimaki and Libarkin 2007). The cosmogenic noble gas isotopes, ^{3}He and ^{21}Ne, are stable, and are used to quantify rates of long-term landscape development (e.g. Margerison et al. 2005). The Atacama Desert is a natural laboratory for testing uplift histories using *in situ* cosmogenic nuclides. The extremely low erosion rates result in exceptionally high concentrations of cosmogenic noble gas isotopes in depositional features (Dunai et al. 2005; Nishiizumi et al. 2005; Kober et al. 2006; Evenstar et al. 2009) and precisely dated volcanic rocks allow constraints to be put on the absolute age of surfaces (Victor et al. 2004; Muñoz and Sepúlveda 1992).

Here we use the concentration of cosmogenic ^{3}He in alluvial boulders from a slowly eroding Miocene-Pliocene-aged surface from the western flank of the Central Andes to test the hypothesis that the Andes mountain belt formed largely in the Late Miocene. Unlike other approaches, this technique is not reliant on complex climate sensitive-altitude relationships and may have potential for application in other mountain belts.

2. Geological background

The western side of the Central Andes can be divided into five different morphotectonic provinces. From west to east these are the Coastal Cordillera, Longitudinal Valley, Precordillera, Western Cordillera and Altiplano. The Coastal Cordillera forms a coastal escarpment rising up from sea-

level to an average elevation of 1000 m. The Longitudinal Valley is a forearc basin filled by Eocene to Miocene sediments derived from the east (Hartley et al. 2000, Pinto et al. 2007). Sedimentation ceased diachronously from middle Miocene to middle Pliocene times, and a relict flat lying Pacific Planation Surface (PPS) developed (Evenstar et al. 2009). The PPS is 30 to 60 km wide with an average elevation of 1000 m. It slopes at 1.5-3° to the west from the Precordillera. The Precordillera ranges in elevation from 1000 to 4000 m, and largely comprises the remnants of a Late Cretaceous to Oligocene magmatic arc blanketed by Early Miocene ignimbrite sheets (Wörner et al. 2002). To the east, the Western Cordillera is a 50 to 100 km wide modern magmatic arc. The Altiplano is a 200 km wide, internally-drained basin at an average elevation of 3.8 km that lies east of the modern arc. The Coastal Cordillera, Longitudinal Valley and part of the Precordillera form an area of extreme aridity due to combination of factors (Hartley 2003). The high aridity leads to some of the lowest erosion rates in the world, and thus to some of the highest concentrations of *in situ* cosmogenic nuclides (Dunai et al. 2005; Kober et al. 2007; Evenstar et al. 2009).

Two general models have been proposed to account for uplift within the Longitudinal Valley and Precordillera on the Western margin of the Andes supporting the end-member scenarios for Andean uplift. Farías et al. (2005) and Hoke et al. (2007) presented evidence for significant uplift in the last 10 million years. Both proposed that the PPS formed at ~10 Ma and suggested that significant incision into the paleosurface was initiated at 10 Ma due to regional tilting, isolating it from the Precordillera. In contrast, Victor et al. (2004) favoured Early Miocene (or earlier) surface uplift generated by movement along a series of reverse faults.

These two surface uplift histories will produce significantly different cosmogenic nuclide concentrations in a non-eroding surface. Late Miocene uplift predicts that for a substantial part of

126 the Miocene the paleosurface was at low elevation receiving lower cosmic ray flux for longer than
127 if the main pulse of uplift had occurred in the Early Miocene. By comparing the predicted
128 concentration of ^{3}He with that measured in alluvial boulders that have been deposited on the
129 paleosurface we can test the timing and rate of uplift of the region.
130
131 **3. *In situ* cosmogenic ^{3}He in boulders from the Pacific Planation Surface**
132
133 Cosmogenic ^{3}He concentrations are used from data published by Evenstar et al. (2009) on
134 measured pyroxene and amphibole separated from twenty-two alluvial boulders of Miocene
135 andesite that sit on the PPS in the Quebrada Aroma area, northern Chile (Figure 1). The boulders
136 were selected on the basis of the absence of evidence of erosion and weathering. Five of the
137 boulders (23/26, 21/26, 22/26, 03/02 and 05/02) from two sites (D and G) have extremely high ^{3}He
138 concentrations for their elevation (Table 1) that are broadly consistent with deposition at the time
139 of, or soon after, formation of the paleosurface (Evenstar et al. 2009). The PPS in Quebrada
140 Aroma is developed on 300 m of alluvial gravels that originate from the Precordillera that overlie
141 the 16.27 ± 0.16 Ma Nama ignimbrite (Member 4 of the Altos de Pica formation) (Pinto et al.
142 2004; Victor et al. 2004; Farías et al. 2005, Pinto et al. 2007). Temporal constraints from dated
143 volcanic rocks and magneto-polarity chronologies from the Camiña Valley, 25 km to the north of
144 the Aroma Quebrada, show that 300 m of alluvium takes 3 to 5 million years to accumulate (Pinto
145 et al. 2004; von Rotz et al. 2005). Using a conservative lower limit of 3 million years for alluvium
146 accumulation, the boulders overlying these sediments cannot have been exposed for more than
147 13.4 million years.
148
149 **4. Uplift history models**
150

151 The measured cosmogenic ^{3}He in the five boulders are compared with concentrations produced in
152 four different surface uplift models for the western flank of the Central Andes (Figure 2).
153 Cosmogenic ^{3}He concentrations are calculated incrementally until present day. Starting elevations
154 vary depending on models (see below) and finish at the current elevation for each site (site G =
155 1,900 m, site D = 1,690 m).
156
157 The following uplift histories have been modelled:
158 *No uplift (NU):* This model assumes that there is no change in elevation from 13.4 Ma until present
159 day.
160 *Early Miocene uplift (EMU):* Uplift rates and times are constructed based on the uplift rates from
161 the adjacent Pica region (Figure 1A) suggested by Victor et al. (2004) with the majority of the
162 uplift occurring prior to 13.4 Ma. The paleoelevation model for both sites show similar surface
163 uplift rates and times of movement as faults within the Pica region (Victor et al. 2004).
164 *Linear Uplift (LU):* This model assumes a linear rate of uplift from sea level at 27 Ma to present
165 day altitudes.
166 *Late Miocene uplift (LMU*): This model is based on rapid uplift during the late Miocene. The
167 timing of elevation change was based on soil carbonate precipitation temperature, oxygen isotopes,
168 fossil-leaf physiognomy and paleosurface reconstruction presented in Hoke et al. (2007) and
169 Garzione et al. (2008). Uplift rates were based on a conservative 800 m of uplift within the
170 Longitudinal Valley in the Late Miocene (Hoke et al. 2007). Background uplift rate of 0.04 mm/yr
171 of the Coastal Cordillera (Dunai et al. 2005) and minor movement along local faults based on
172 Farías et al. (2005) were assumed to have operated from 13.4 Ma to the present day.
173
174 For each uplift history the three main *in situ* cosmogenic nuclide scaling models were used (Lal
175 1991, Dunai 2000, Lifton et al. 2014). Palaeomagnetic data from northern Chile indicate that there

has been no latitudinal translation of strata since the late Palaeozoic (Jesinkey et al. 1987; Hartley et al. 1988; Somoza & Tomlinson 2002), so it is not necessary to calculate changes in production rate with latitude. Variation in the geomagnetic field strength through time can affect the long-term production rates of cosmogenic nuclides especially at low latitudes. Fluctuations on time scales longer than 100 kyr or so tend to be averaged out.

We have used the weighted mean of the cosmogenic ^{3}He production rate in olivine compiled by Goehring et al. (2010), and incorporated more recent measurements (Foeken et al. 2012; Blard et al. 2013). The sea level high latitude ^{3}He production rates used for the three scaling factors are 119.3 ± 3.0 atoms/g for Lal (1991), 121.2 ± 3.2 atoms/g for Dunai (2000) and 114.6 ± 3.0 atoms/g for Lifton et al. (2014). These were scaled for the composition of the analysed minerals using the element production rates of Masarik (2002). The contribution of ^{3}He produced by cosmogenic thermal neutrons (CTN) on ^{6}Li cannot be ignored (Dunai et al. 2007). Lithium in andesites is relatively low (<20 ppm) and due to mineral-melt partitioning coefficients it resides predominately in the matrix, with pyroxenes displaying concentrations usually below 2 ppm. However amphiboles typically have higher Li contents and CTN-derived cosmogenic ^{3}He can contribute up to 40% of total (Amidon et al. 2012). Li was measured in the 3 amphibole samples using LAICPMS techniques (see Supporting information). It ranges from 23 - 49 ppm and accounts for 6-12% of that produced by spallation (see Supporting information).

5. Results

The cosmogenic ^{3}He produced by spallation at each site, for each surface uplift scenario and scaling factors (Table 2), are plotted in Figure 3. It is important to stress that these modelled values are upper limits on the amount of cosmogenic He that has been produced as it assumes a

maximum possible surface exposure age and does not take into account the effect of erosion, burial or exhumation of the boulders during their residence on the surface. The spallation-produced cosmogenic ^{3}He concentrations of each mineral sample are plotted as dashed lines on Figure 3. Correction for CTN-cosmogenic He has been made using measured Li in amphibole (Table S3) and an upper limit of 5% for the pyroxenes which equates to 20 ppm Li (Dunai et al. 2007, Amidon et al. 2012).

The rapid Late Miocene uplift history predicts the lowest cosmogenic ^{3}He concentrations (2.1 to 2.8 x 10^{9} atoms/g) as the surfaces have spent the shortest time at high elevation. Cosmogenic ^{3}He concentrations are predicted to be highest in samples that remained at the current elevation throughout their history (3.2 to 4.2 x 10^{9} atoms/g). Uplift in the Early Miocene gives concentrations in the range 2.6 to 3.4 x 10^{9} atoms/g, while linear uplift produces cosmogenic ^{3}He concentrations of 2.4 to 3.1 x 10^{9} atoms/g. The scaling factors of Dunai (2000) systematically yield the lowest cosmogenic ^{3}He concentrations, while those of Lal (1991) produce the highest.

The Late Miocene uplift model generates maximum ^{3}He concentrations that are lower than measured in all samples using all scaling factors (Figure 3). The samples contain 0.2 – 1.3 x 10^{9} atoms ^{3}He/g more ^{3}He than Late Miocene Uplift predicts depending on scaling scheme.

All samples except 23/26 have ^{3}He concentrations that are predicted by a no uplift history or Early Miocene uplift. The cosmogenic ^{3}He concentration predicted by Linear uplift using Lal (1991) scaling factors is higher than measured in the samples, except for sample 23/26. The $^{3}He_{cos}$ concentration measured in boulder 23/26 overlaps that predicted for no uplift of the surface using the Lal (1991) or Lifton et al. (2014) scaling factors.

6. Discussion

6.1 Ruling out Late Miocene uplift

The principal aim of this work is to test whether or not the high concentrations of $^{3}He_{cos}$ previously measured in alluvial boulders from Querada Aroma (Evenstar et al. 2009) can be accounted for by surface uplift in the Late Miocene. The simple comparison with predicted $^{3}He_{cos}$ concentrations clearly appears to exclude Late Miocene uplift (Figure 3).

The boulders on the desert pavement may have undergone small degrees of erosion, suffered exhumation and/or partial burial. All of these processes would decrease the cosmogenic He production rate and therefore yield lower concentrations compared to that produced by complete exposure. The effect of erosion is documented in the supporting information (Figure S3). Using a low erosion rate of 1cm/myr shows how even a minor amount of erosion would greatly decrease the modelled concentrations. When comparing these modelled concentrations to measured $^{3}He_{cos}$ in the alluvial boulders only assuming that no uplift had occurred over the last 13.4 Ma would be consistent with the data. As such erosional processes would lend support to an even earlier uplift model.

Pre-exposure of all the boulders prior to deposition on the PPS is the only process that could have increased the concentration of cosmogenic He. There are a number of reasons why a significant contribution of inheritance cannot account for the excess helium within the samples assuming Late Miocene Uplift.

Firstly, the similarity of the ^{3}He concentration in 4 of the 5 samples, relative to elevation, is not typical of inheritance (Dunai et al. 2005, Nishiizumi et al. 2005, Kober et al. 2007, Fujioka et al. 2005, Blisniuk et al. 2012, Van der Wateren and Dunai, 2001). It would require that each boulder has had a similar pre-exposure history and that each was deposited with the pre-exposed surface at the top of the boulder.

Secondly, the boulders on the PPS are located on the flat lying paleosurface, which is 60 km wide and slopes at an angle of 1.5° (Figure 1). The nearest significant large scarps for boulders to originate is over 20 km to the east. The boulders could only have moved in a large fluvial event originating within the Precordillera. Late Miocene uplift requires the isolation of the PPS at 10 Ma due to increased incision between the PPS and Precordillera. Therefore the boulders on the PPS could only obtain significant pre-exposure from higher elevations prior to 10 Ma. At this time the elevation of the Precordillera and Western Cordillera were significantly lower than currently; the highest elevation is predicted to be ~3500 m (Garzoine et al. 2008). This makes accounting for the excess He within the samples highly unlikely. For instance, the excess $^{3}He_{cos}$ in boulder 23/26 relative to that predicted by Late Miocene uplift at 13.2 Ma ($> 1 \times 10^{9}$ atoms/g) is equivalent to ~13 million years exposure at sea level, or 3 million years exposure at the current altitude of Quebrada Aroma. The excess He requires pre-exposure for a minimum of ~1.5 million years at the highest possible elevation within the paleo-Andes prior to 13.4 Ma, assuming no surface erosion. The current erosion rate in the Western Cordillera is between 100 and 1000 cm/Myr at similar elevations (Kober et al. 2007). Such high erosion rates are not conducive to preservation of enough cosmogenic He to account for the apparent excess.

In summary, it is unlikely that the PPS boulders have experienced significant pre-exposure thus the measured cosmogenic He reflects the surface uplift history. The Late Miocene uplift model cannot

produce enough cosmogenic ^{3}He to account for the concentrations measured in the alluvial boulders from the PPS. The data do not constrain a single unique uplift history, but the data appear to require that the majority of the uplift occurred prior to the Late Miocene.

6.2 Implications for Andean uplift

Determining accurately the time of the onset of surface uplift throughout the Central Andes is essential for understanding the geodynamic mechanisms of plateau development at convergent continental margins, and will help inform orogenic erosion, sedimentation, local and regional climate and rainfall patterns (Barnes and Ehlers 2009). The results presented here suggest that the PPS obtained a substantial proportion of its elevation prior to 13.4 Ma. This is consistent with either an early phase of uplift in the Early Miocene with relatively minor uplift after or relatively slow constant surface uplift rates for the western flank of the Andean Cordillera from 30 Ma or earlier.

This is independent of climate sensitive-altitude relationships, and stands in marked contrast to previous studies that utilised oxygen isotopes (Garzione et al. 2006), clumped C-O isotopes (Ghosh et al. 2006; Quade et al. 2007) and fluvial incision rate (Schildgen et al. 2007; Hoke et al. 2007; Thouret et al. 2007) that suggest the majority of uplift occurred after 10 Ma. The results presented here fit the structural, surface incision, deformation/exhumation history and timing of sedimentary deposition that indicate progressive surface uplift associated with crustal shortening from the Late Eocene or earlier (Victor et al. 2004, McQuarrie et al. 2005, Hoke and Lamb 2007, Ehler and Poulsen 2009). This is in contrast to the sudden, rapid uplift in the Late Miocene that is associated with delamination of an overthickened orogenic crustal root (e.g. Garzione et al. 2008). These observations suggest that large mountain chains can be created within ocean-continent

subduction zone settings by progressive shortening and thickening of continental crust and without the need for large-scale mantle delamination.

Acknowledgements

This material is based upon work supported by NERC grant (NER/S/A/2003/11945) and BHP Billiton. Data used in this study are provided from Evenstar et al. (2009) and from modelling detailed in the auxiliary material. We are grateful to Philip G. Roxby, Steve Sparks and Shasta Marrero for help with preparation of the manuscript.

References

Amidon, W.H. & Farley, K.A. (2012) Cosmogenic ^{3}He and ^{21}Ne dating of biotite and hornblende. Earth Planet. Sci. Lett.,, 313–314, 86-94, doi:10.1016/J.Epsl.2011.11.005.

Barke, R., and S. Lamb (2006), Late Cenozoic uplift of the Eastern Cordillera, Bolivian Andes, Earth Planet. Sci. Lett., 249(3-4), 350-367, doi:10.1016/J.Epsl.2006.07.012.

Barnes, J. B., and T. A. Ehlers (2009), End member models for Andean Plateau uplift, Earth-Sci. Rev., 97(1-4), 105-132, doi:10.1016/J.Earscirev.2009.08.003.

Blard, P. H., J. Lavé, F. Sylvestre, C. J. Placzek, C. Claude, V. Galy, T. Condom, and B. Tibari (2013), Cosmogenic ^{3}He production rate in the high tropical Andes (3800 m, 20°S): Implications for the local last glacial maximum, Earth Planet. Sci. Lett., 377–378, 260-275, doi: 10.1016/j.epsl.2013.07.006.

326 Blisniuk, K., M. Oskin, K. Fletcher, T. Rockwell, and W. Sharp (2012), Assessing the reliability of
327 U-series and ^{10}Be dating techniques on alluvial fans in the Anza Borrego Desert, California, Quat.
328 Geochron., 13, 26-41, doi:10.1016/j.quageo.2012.08.004.
329
330 Clift, P. D. (2010), Enhanced global continental erosion and exhumation driven by Oligo-
331 Miocene climate change, Geophys. Res. Lett. 37(9), L09402, doi:10.1029/2010GL043067.
332
333 Dunai, T. J. (2000), Scaling factors for production rates of *in situ* produced cosmogenic nuclides: a
334 critical reevaluation, Earth Planet. Sci. Lett., 176(1), 157-169, doi:10.1016/S0012-821x(99)00310-
335 6.
336
337 Dunai, T. J. (2001), Influence of secular variation of the geomagnetic field on production rates of
338 *in situ* produced cosmogenic nuclides, Earth Planet. Sci. Lett., 193(1-2), 197-212,
339 doi:10.1016/S0012-821x(01)00503-9.
340
341 Dunai, T. J., G. A. G. Lopez, and J. Juez-Larre (2005), Oligocene-Miocene age of aridity in the
342 Atacama Desert revealed by exposure dating of erosion-sensitive landforms, Geology, 33(4), 321-
343 324, doi:10.1130/G21184.1.
344
345 Dunai, T. J., F. M. Stuart, R. Pik, P. Burnard, and E. Gayer (2007), Production of ^{3}He in crustal
346 rocks by cosmogenic thermal neutrons, Earth Planet. Sci. Lett., 258(1-2), 228-236,
347 doi:10.1016/J.Espl.2007.03.031.
348
349 Ehlers, T. A., and C. J. Poulsen (2009), Influence of Andean uplift on climate and paleoaltimetry
350 estimates, Earth Planet. Sci. Lett., 281(3-4), 238-248, doi:10.1016/j.epsl.2009.02.026.
351
352 Evenstar, L. A., A. J. Hartley, F. M. Stuart, A. E. Mather, C. M. Rice, and G. Chong (2009),

353 Multiphase development of the Atacama Planation Surface recorded by cosmogenic ^{3}He exposure
354 ages: Implications for uplift and Cenozoic climate change in western South America, Geology,
355 37(7), 658-658, doi:10.1130/G25437A.1.
356
357 Farías, M., R. Charrier, D. Comte, J. Martinod, and G. Hérail (2005), Late Cenozoic deformation
358 and uplift of the western flank of the Altiplano: Evidence from the depositional, tectonic, and
359 geomorphologic evolution and shallow seismic activity (northern Chile at 19°30′S), Tectonics,
360 24(4), TC4001, doi:10.1029/2004tc001667.
361
362 Foeken, J. P. T., F. M. Stuart, and D. F. Mark (2012), Long-term low latitude cosmogenic He-3
363 production rate determined from a 126 ka basalt from Fogo, Cape Verdes, Earth Planet. Sci. Lett.,
364 359, 14-25, doi:10.1016/J.Epsl.2012.10.005.
365
366 Fujioka, T., J. Chappell, M. Honda, I. Yatsevich, K. Fifield, and D. Fabel (2005), Global cooling
367 initiated stony deserts in central Australia 2–4 Ma, dated by cosmogenic ^{21}Ne-^{10}Be, Geology,
368 33(12), 993-996, doi:10.1130/g21746.1.
369
370 Garzione, C. N., G. D. Hoke, J. C. Libarkin, S. Withers, B. MacFadden, J. Eiler, P. Ghosh, and A.
371 Mulch (2008), Rise of the Andes, Science, 320(5881), 1304-1307, doi:10.1126/science.1148615.
372
373 Garzione, C. N., P. Molnar, J. C. Libarkin, and B. J. MacFadden (2006), Rapid late Miocene rise
374 of the Bolivian Altiplano: Evidence for removal of mantle lithosphere, Earth Planet. Sci. Lett.,
375 241(3-4), 543-556, doi:10.1016/j.epsl.2005.11.026.
376
377 Ghosh, P., C. N. Garzione, and J. M. Eiler (2006), Rapid uplift of the Altiplano revealed through

^{13}C-^{18}O bonds in paleosol carbonates, Science, 311(5760), 511-515, doi:10.1126/Science.1119365.

Goehring, B. M., M. D. Kurz, G. Balco, J. M. Schaefer, J. Licciardi, and N. Lifton (2010), A reevaluation of *in situ* cosmogenic ^{3}He production rates, Quat. Geochron., 5(4), 410-418, doi:10.1016/J.Quageo.2010.03.001.

Gregory-Wodzicki, K. M. (2000), Uplift history of the Central and Northern Andes: A review, Geol. Soc. Am. Bull., 112(7), 1091-1105, doi:10.1130/0016-7606(2000)112<1091:Uhotca>2.3.Co;2.

Hartley, A. J. (2003), Andean uplift and climate change, J. Geol. Soc. London, 160, 7-10, doi:10.1144/0016-764902-083.

Hartley, A. J., and L. Evenstar (2010), Cenozoic stratigraphic development in the north Chilean forearc: Implications for basin development and uplift history of the Central Andean margin, Tectonophysics, 495(1-2), 67-77, doi:10.1016/j.tecto.2009.05.013.

Hartley, A. J., G. May, G. Chong, P. Turner, S. J. Kape, and E. J. Jolley (2000), Development of a continental forearc: A Cenozoic example from the Central Andes, northern Chile, Geology, 28(4), 331-334, doi:10.1130/0091-7613(2000)28<331:Doacfa>2.0.Co;2.

Hartley, A. J., T. Sempere, and G. Wörner (2007), A comment on "Rapid late Miocene rise of the Bolivian Altiplano: Evidence for removal of mantle lithosphere" by C.N. Garzione et al. [Earth Planet. Sci. Lett. 241 (2006) 543-556], Earth Planet. Sci. Lett., 259(3-4), 625-629, doi:10.1016/J.Epsl.2007.04.012.

Hartley, A. J., P. Turner, G. D. Williams, and S. Flint (1988), Palaeomagnetism of the Cordillera de la Costa, northern Chile: evidence for local forearc rotation, Earth Planet. Sci. Lett., 89(3–4),

375-386, doi:10.1016/0012-821X(88)90124-0.

Hoke, G. D., and C. N. Garzione (2008), Paleosurfaces, paleoelevation, and the mechanisms for the late Miocene topographic development of the Altiplano plateau, Earth Planet. Sci. Lett., 271(1-4), 192-201, doi:10.1016/J.Epsl.2008.04.008.

Hoke, G. D., B. L. Isacks, T. E. Jordan, N. Blanco, A. J. Tomlinson, and J. Ramezani (2007), Geomorphic evidence for post-10 Ma uplift of the western flank of the central Andes 18°30′-22°S, Tectonics, 26(5), TC5021, doi:10.1029/2006tc002082.

Hoke, L., and S. Lamb (2007), Cenozoic behind-arc volcanism in the Bolivian Andes, South America: implications for mantle melt generation and lithospheric structure, J. Geol. Soc. London, 164, 795-814, doi:10.1144/0016-76492006-092.

Ivy-Ochs, S., C. Schlüchter, P. W. Kubik, B. Dittrich-Hannen, and J. Beer (1995), Minimum ^{10}Be exposure ages of early Pliocene for the Table Mountain plateau and the Sirius Group at Mount Fleming, Dry Valleys, Antarctica, Geology, 23(11), 1007-1010, doi:10.1130/0091-7613(1995)023<1007:mbeaoe>2.3.co;2.

Jeffery, M. L., T. A. Ehlers, B. J. Yanites, and C. J. Poulsen (2013), Quantifying the role of paleoclimate and Andean Plateau uplift on river incision, J. Geophys. Res.: Earth Surface, 118(2), 852-871, doi:10.1002/jgrf.20055.

Jesinkey, C., R. D. Forsythe, C. Mpodozis, and J. Davidson (1987), Concordant late Paleozoic paleomagnetizations from the Atacama Desert: implications for tectonic models of the Chilean

Andes, Earth Planet. Sci. Lett., 85(4), 461-472, doi:10.1016/0012-821X(87)90141-5.

Jordan, T. E., B. L. Isacks, R. W. Allmendinger, J. A. Brewer, V. A. Ramos, and C. J. Ando (1983), Andean tectonics related to geometry of subducted Nazca Plate, Geol. Soc. Am. Bull., 94(3), 341-361, doi:10.1130/0016-7606(1983)94<341:Atrtgo>2.0.Co;2.

Jordan, T. E., P. L. Nester, N. Blanco, G. D. Hoke, F. Davila, and A. J. Tomlinson (2010), Uplift of the Altiplano-Puna plateau: A view from the west, Tectonics, 29(5), TC5007 doi:10.1029/2010tc002661.

Kay, S. M., B. Coira, and J. Viramonte (1994), Young mafic back arc volcanic-rocks as Indicators of continental lithospheric delamination beneath the Argentine Puna Plateau, Central Andes, J Geophys. Res.-Solid Earth, 99(B12), 24323-24339, doi:10.1029/94jb00896.

Kober, F., S. Ivy-Ochs, F. Schlunegger, H. Baur, P. W. Kubik, and R. Wieler (2007), Denudation rates and a topography-driven rainfall threshold in northern Chile: Multiple cosmogenic nuclide data and sediment yield budgets, Geomorph., 83(1-2), 97-120, doi:10.1016/j.geomorph.2006.06.029.

Kober, F., F. Schlunegger, G. Zeilinger, and H. Schneider (2006), Surface uplift and climate change: The geomorphic evolution of the Western Escarpment of the Andes of northern Chile between the Miocene and present, Geol. S. Am. Bull., 398, 75-86, doi:10.1130/2006.2398(05).

Lal, D. (1991), Cosmic ray labeling of erosion surfaces: *in situ* nuclide production rates and erosion models, Earth Planet. Sci. Lett., 104(2–4), 424-439, doi:10.1016/0012-821X(91)90220-C.

457

458 Lamb, S., and L. Hoke (1997), Origin of the high plateau in the Central Andes, Bolivia, South
459 America, Tectonics, 16(4), 623-649, doi:10.1029/97tc00495.
460

461 Lifton, N., T. Sato, and T. J. Dunai (2014), Scaling *in situ* cosmogenic nuclide production rates
462 using analytical approximations to atmospheric cosmic-ray fluxes, Earth Planet. Sci. Lett., 386(0),
463 149-160, doi:10.1016/j.epsl.2013.10.052.
464

465 Margerison, H.R., Phillips, W.M., Stuart, F.M., and Sugden, D.E. (2005). Cosmogenic ^{3}He
466 concentrations in ancient flood deposits from the Coombs Hills, northern Dry Valleys, East
467 Antarctica: interpreting exposure ages and erosion rates. Earth and Planet. Sci. Lett., 230, 163-175,
468 doi:10.1016/j.epsl.2004.11.007
469

470 Masarik, J. (2002), Numerical simulation of *in-situ* production of cosmogenic nuclides, Geochim.
471 Cosmochim. Acta, 66(15A), A491-A491, doi:10.1016/j.nimb.2007.03.003
472

473 McQuarrie, N. (2002), The kinematic history of the central Andean fold-thrust belt, Bolivia:
474 Implications for building a high plateau, Geol. Soc. Am. Bull., 114(8), 950-963, doi:10.1130/0016-
475 7606(2002)114<0950:Tkhotc>2.0.Co;2.
476

477 Molnar, P., and C. N. Garzione (2007), Bounds on the viscosity coefficient of continental
478 lithosphere from removal of mantle lithosphere beneath the Altiplano and Eastern Cordillera,
479 Tectonics, 26(2), TC2013, doi:10.1029/2006TC001964
480

481 Montgomery, D. R., G. Balco, and S. D. Willett (2001), Climate, tectonics, and the morphology of

the Andes, Geology, 29(7), 579-582, doi:10.1130/0091-7613(2001)029<0579:Ctatmo>2.0.Co;2.

Muñoz, N., Sepúlveda, p. (1992), Estructuras compresivas convergencia al Oeste en el borde oriental de la Depresión Central (19°15' lat. Sur), Rev. Geol. Chile, 19, 214-247, doi:10.5027/andgeoV19n2-a07

Munoz, N., and R. Charrier (1996), Uplift of the western border of the Altiplano on a west-vergent thrust system, Northern Chile, J. S. Am. Earth Sci., 9(3-4), 171-181, doi:10.1016/0895-9811(96)00004-1.

Nishiizumi, K., M. W. Caffee, R. C. Finkel, G. Brimhall, and T. Mote (2005), Remnants of a fossil alluvial fan landscape of Miocene age in the Atacama Desert of northern Chile using cosmogenic nuclide exposure age dating, Earth Planet. Sci. Lett., 237(3–4), 499-507, doi:10.1016/j.epsl.2005.05.032.

Picard, D., T. Sempere, and O. Plantard (2008), Direction and timing of uplift propagation in the Peruvian Andes deduced from molecular phylogenetics of highland biotaxa, Earth Planet. Sci. Lett., 271(1-4), 326-336, doi:10.1016/j.epsl.2008.04.024.

Pinto, L., Hérail, G., Charrier, R. (2004), Syntectonic sedimentation associated with Neogene structures in the Precordillera of Moquella Zone, Tarapacá (19°15'S, northern Chile), Rev. Geol. Chile, 31, 19-44, doi:10.4067/S0716-02082004000100002.

Pinto, L., Hérail, G., Fontan, F. & De Parseval, P. (2007), Neogene erosion and uplift of the western edge of the Andean plateau as determined by detrital heavy mineral analysis, Sed. Geol., 195, 217-237,

507 doi;10.1016/j.sedgeo.2006.08.001.
508
509 Quade, J., C. Garzione, and J. Eiler (2007), Paleoelevation Reconstruction using Pedogenic
510 Carbonates, Rev. Mineral. Geochem., 66(1), 53-87, doi:10.2138/rmg.2007.66.3.
511
512 Riihimaki, C. A., and J. C. Libarkin (2007), Terrestrial cosmogenic nuclides as paleoaltimetric
513 proxies, Rev. Mineral. Geochem., 66, 269-278, doi:10.2138/Rmg.2007.66.11.
514
515 Rosenbaum, G., D. Giles, M. Saxon, P. G. Betts, R. F. Weinberg, and C. Duboz (2005),
516 Subduction of the Nazca Ridge and the Inca Plateau: Insights into the formation of ore deposits in
517 Peru, Earth Planet. Sci. Lett., 239(1-2), 18-32, doi:10.1016/J.Epsl.20005.08.003.
518
519 Schildgen, T. F., K. V. Hodges, K. X. Whipple, P. W. Reiners, and M. S. Pringle (2007), Uplift of
520 the western margin of the Andean plateau revealed from canyon incision history, southern Peru,
521 Geology, 35(6), 523, doi:10.1130/g23532a.1.
522
523 Sempere, T., R. F. Butler, D. R. Richards, L. G. Marshall, W. Sharp, and C. C. Swisher (1997),
524 Stratigraphy and chronology of upper Cretaceous lower Paleogene strata in Bolivia and northwest
525 Argentina, Geol. Soc. Am. Bull., 109(6), 709-727, doi:10.1130/0016-
526 7606(1997)109<0709:Sacouc>2.3.Co;2.
527
528 Silver, P. G., R. M. Russo, and C. Lithgow-Bertelloni (1998), Coupling of South American and
529 African Plate motion and Plate deformation, Science, 279(5347), 60-63,
530 doi:10.1126/Science.279.5347.60.
531

Somoza, R., and A. Tomlinson (2002), Paleomagnetism in the Precordillera of northern Chile (22°30'S): implications for the history of tectonic rotations in the Central Andes, Earth Planet. Sci. Lett., 194(3–4), 369-381, doi:10.1016/S0012-821X(01)00548-9.

Thouret, J. C., G. Wörner, Y. Gunnell, B. Singer, X. Zhang, and T. Souriot (2007), Geochronologic and stratigraphic constraints on canyon incision and Miocene uplift of the Central Andes in Peru, Earth Planet. Sci. Lett., 263(3-4), 151-166, doi:10.1016/j.epsl.2007.07.023.

Van der Wateren, F. M., and T. J. Dunai (2001), Late Neogene passive margin denudation history—cosmogenic isotope measurements from the central Namib desert, Global Planet. Change, 30(3–4), 271-307, doi:10.1016/S0921-8181(01)00104-7.

Victor, P., O. Oncken, and J. Glodny (2004), Uplift of the western Altiplano plateau: Evidence from the Precordillera between 20° and 21°S (northern Chile), Tectonics, 23(4), TC4004, doi:10.1029/2003tc001519.

von Rotz, R., Schlunegger, F., Heller, F., Villa, I. (2005), Assessing the age of relief growth in the Andes of northern Chile: magneto-polarity chronologies from Neogene continental sections, Terra Nova, 17, 462-471, doi:10.1111/j.1365-3121.2005.00634.x

Wörner, G., D. Uhlig, I. Kohler, and H. Seyfried (2002), Evolution of the West Andean Escarpment at 18°S (N. Chile) during the last 25 Ma: uplift, erosion and collapse through time, Tectonophysics, 345(1–4), 183-198, doi:10.1016/S0040-1951(01)00212-8.

Figures

Figure 1; A) Location of study area in the Atacama Desert (DEM based on GTOPO30). The Pacific planation surface is located within the dashed line. Boxes show the location of the Aroma Quebrada and Pica region area studied by Victor et al. (2004). **B)** Landsat image of the Aroma Quebrada with location of samples. Soga Flexure, Aroma Flexure, Calacala Flexure were mapped by Farías et al. (2005). Faults A – E are identified from landsat images. **C)** Photographs of the Pacific planation surface with rounded alluvial/fluvial boulders, **D)** Sample 03/02 and **E)** sample 05/02.

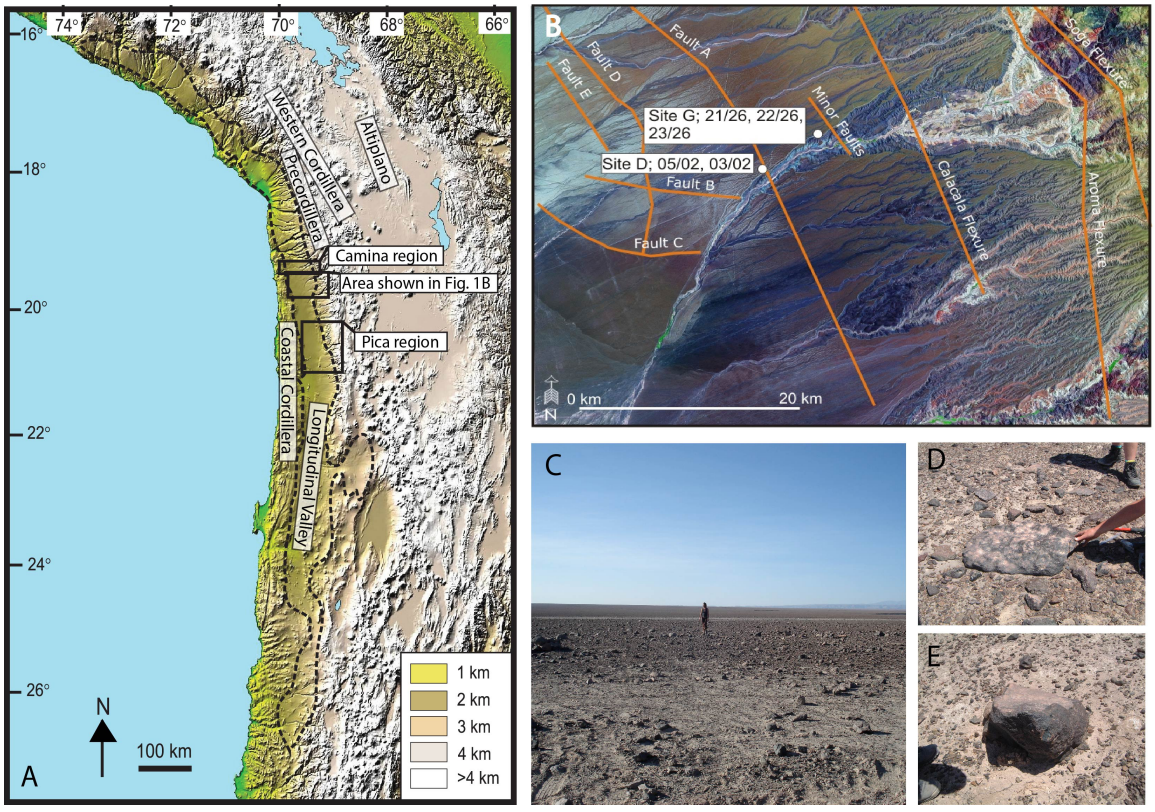

Figure 2; The paleoelevation histories since 14 Ma for site G (elevation 1900 m) and D (elevation 1690m) used in this study. No uplift (NU), orange; Early Miocene uplift (EMU), green; Linear

571 uplift (LU), blue; Late Miocene uplift (LMU), red.

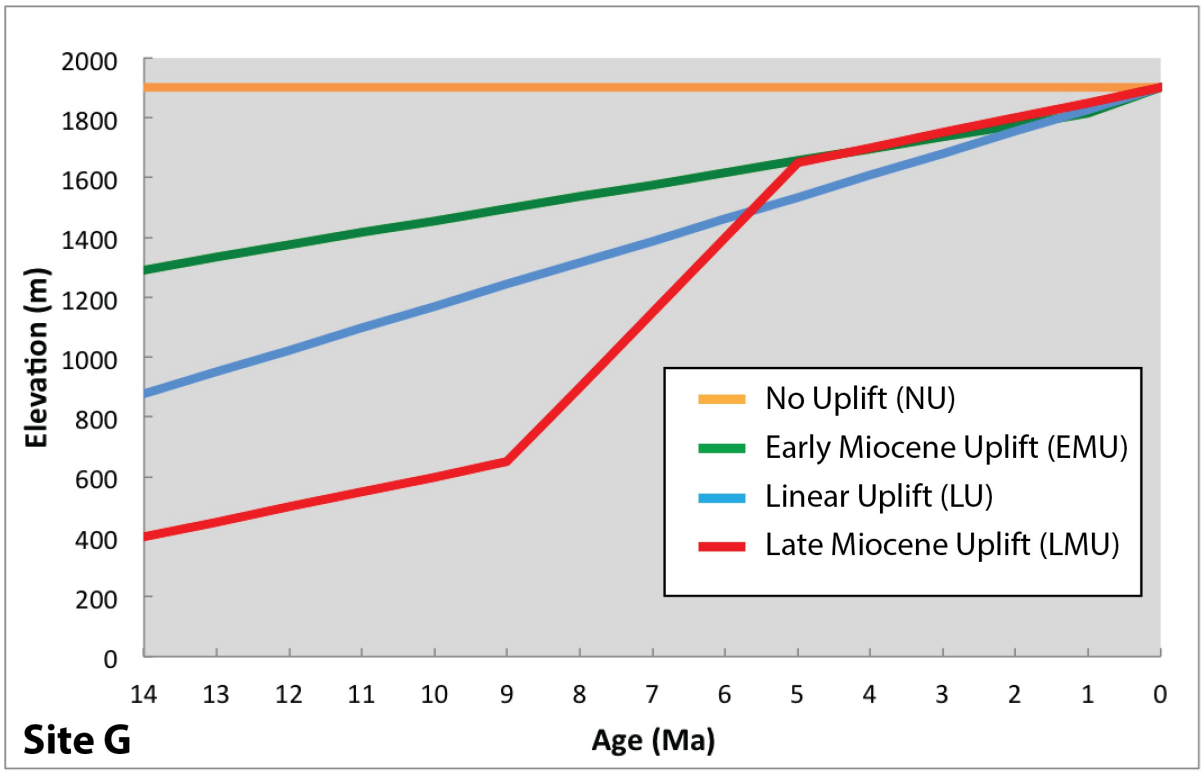

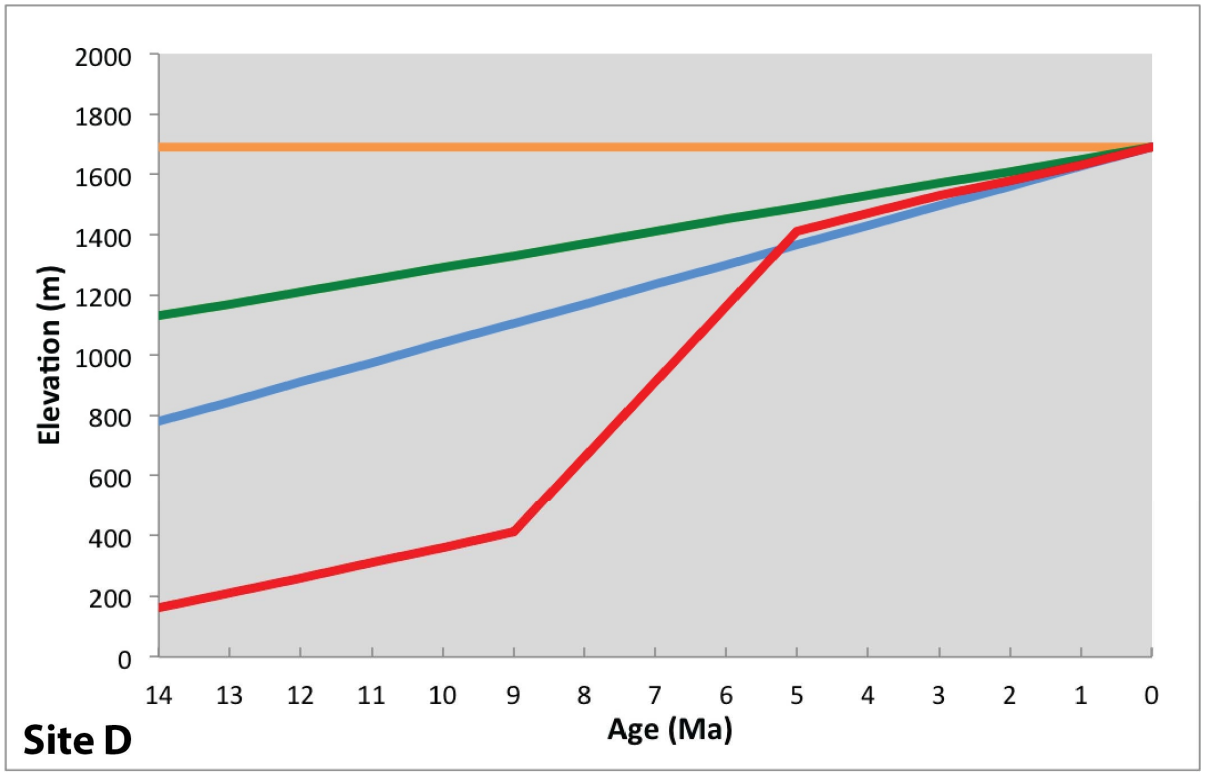

572

573 **Figure 3;** Concentration of cosmogenic ^{3}He calculated for different uplift histories for two sites in
574 Quebrada Aroma, northern Chile. Three scaling factor algorithms were considered; circle, Lal
575 (1991), circle, Dunai (2000), square, and Lifton et al. (2014), triangle. Symbols represents the ^{3}He
576 concentrations (atoms/g) for the four uplift scenarios (colours as per Figure 2). The horizontal
577 dashed lines represent the He concentration of each sample.

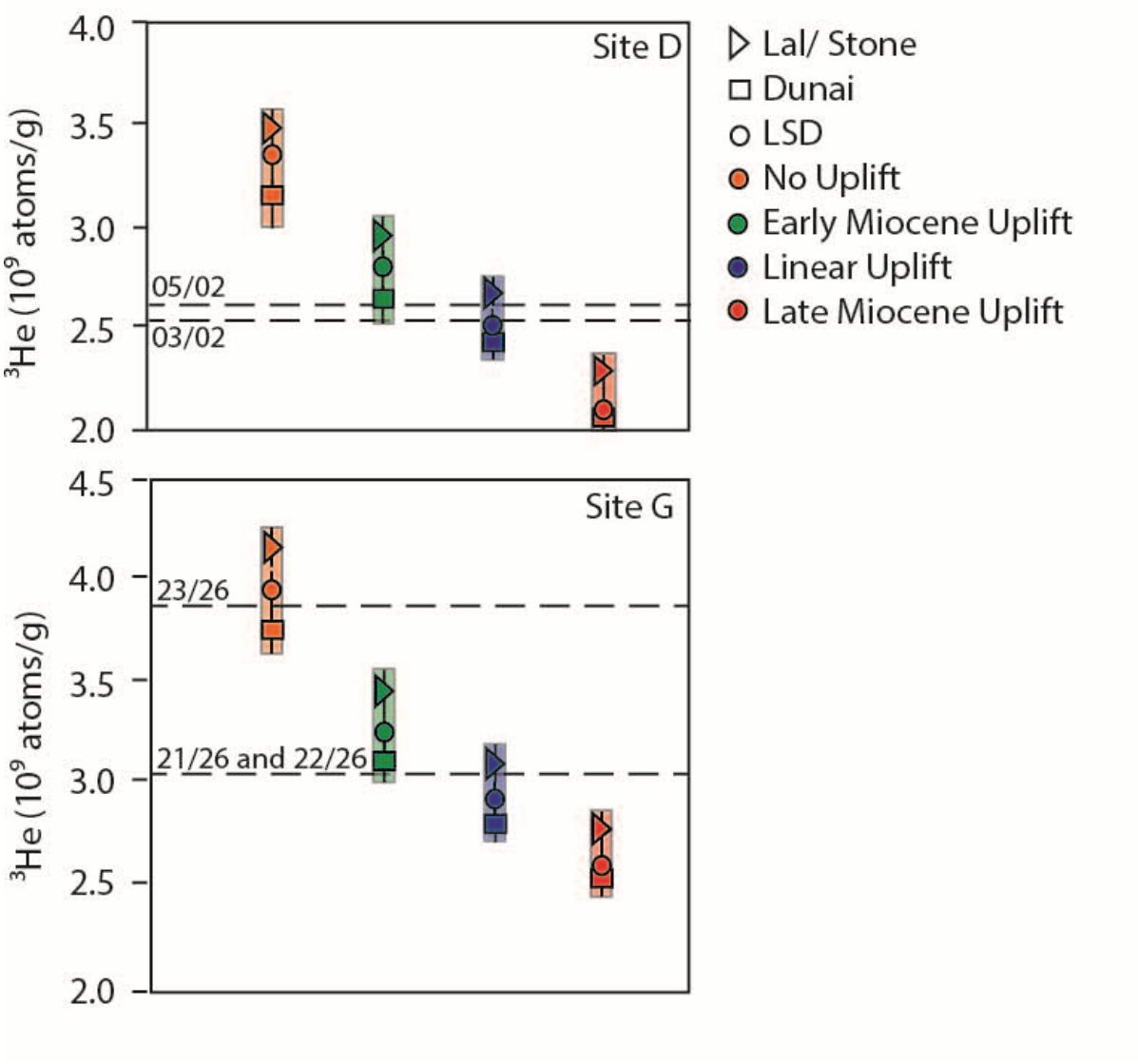

578

579 **Table 1.** Concentration of ^{3}He in alluvial boulders from the Quebrada Aroma region after Evenstar
580 et al. (2009) reduced to account for ^{3}He contribution from neutron capture on Li.

581

Site	Altitude	Sample	^{3}He (10^{9} atoms/g)
G	1900	21/26	3.03 ± 0.095
		22/26	3.04 ± 0.096
		23/26	3.87 ± 0.030
D	1690	03/02	2.54 ± 0.049
		05/02	2.64 ± 0.036

582

583 **Table 2.** Modelled maximum ^{3}He concentrations* produced in boulders from Quebrada Aroma, northern Chile.

584

Site	No uplift			Early Miocene uplift			Linear uplift			Late Miocene uplift		
	Lal (1991)	**Dunai (2000)**	**Lifton et al. (2014)**	**Lal (1991)**	**Dunai (2000)**	**Lifton et al. (2014)**	**Lal (1991)**	**Dunai (2000)**	**Lifton et al. (2014)**	**Lal (1991)**	**Dunai (2000)**	**Lifton et al. (2014)**
G	4.15 ± 0.11	3.76 ± 0.13	3.95 ± 0.12	3.43 ± 0.10	3.11 ± 0.09	3.25 ± 0.09	3.07 ± 0.08	2.80 ± 0.09	2.91 ± 0.08	2.78 ± 0.08	2.53 ± 0.08	2.58 ± 0.07
D	3.48 ± 0.08	3.16 ± 0.12	3.32 ± 0.10	2.94 ± 0.08	2.64 ± 0.08	2.80 ± 0.08	2.65 ± 0.07	2.42 ± 0.07	2.50 ± 0.08	2.30 ± 0.06	2.09 ± 0.06	2.12 ± 0.06

585

586 * All values are 10^{9} atoms/g

587

74°
72°
70°
68°
66°
16°
18°
20°
22°
24°
26°
Western Cordillera
Precordillera
Altiplano
Camina region
Area shown in Fig. 1B
Pica region
Coastal Cordillera
Longitudinal Valley
1 km
2 km
3 km
4 km
>4 km
N
100 km
A
B
Fault A
Fault D
Fault E
Fault B
Fault C
Site G; 21/26, 22/26, 23/26
Site D; 05/02, 03/02
Minor Faults
Calacala Flexure
Soga Flexure
Aroma Flexure
N
0 km
20 km
C
D
E

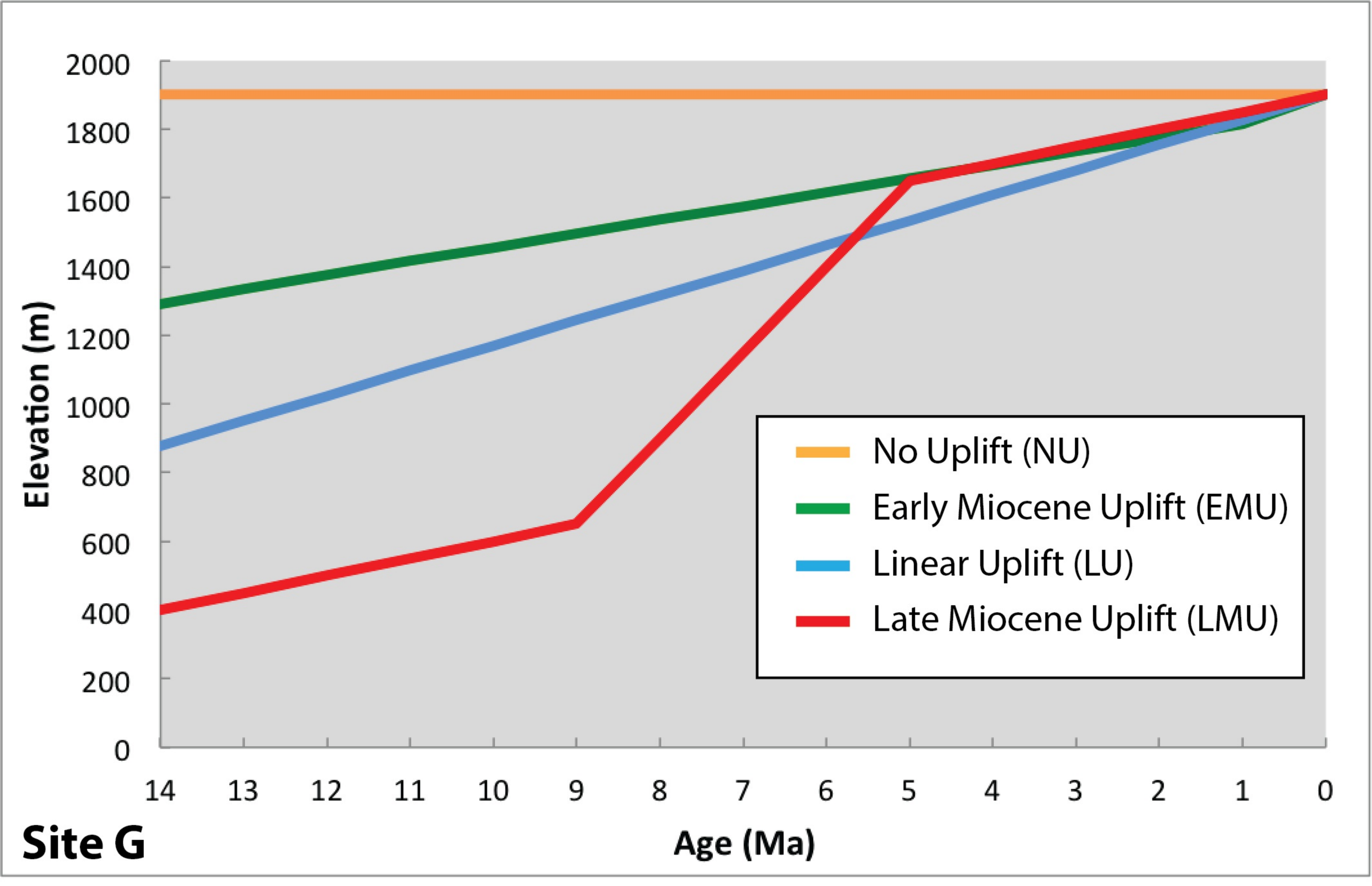
2000
1800
1600
1400
1200
1000
800
600
400
200
0
Elevation (m)
14
13
12
11
10
9
8
7
6
5
4
3
2
1
0
Age (Ma)
No Uplift (NU)
Early Miocene Uplift (EMU)
Linear Uplift (LU)
Late Miocene Uplift (LMU)
Site G

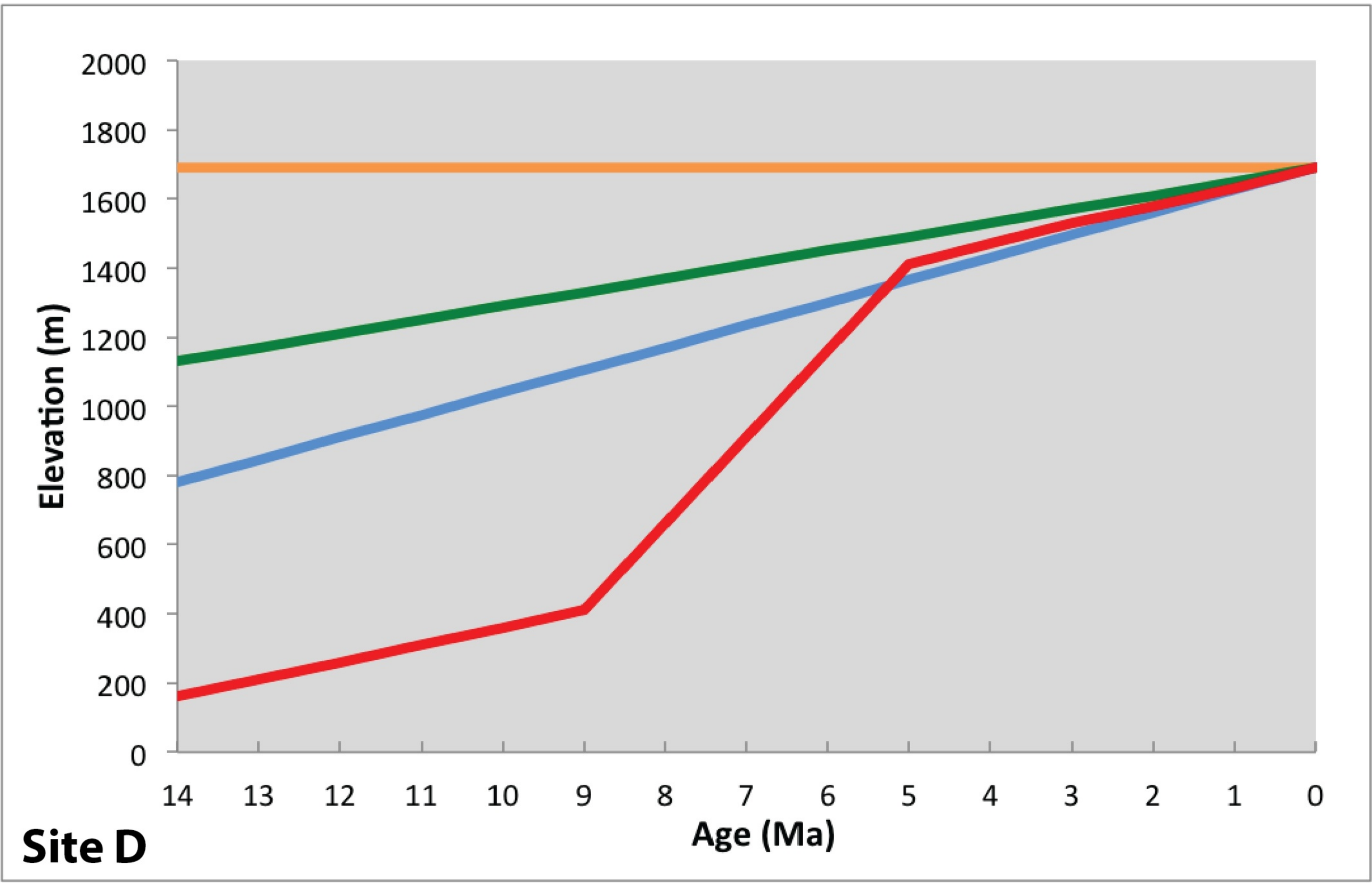
2000
1800
1600
1400
1200
1000
800
600
400
200
0
Elevation (m)
14
13
12
11
10
9
8
7
6
5
4
3
2
1
0
Age (Ma)
Site D

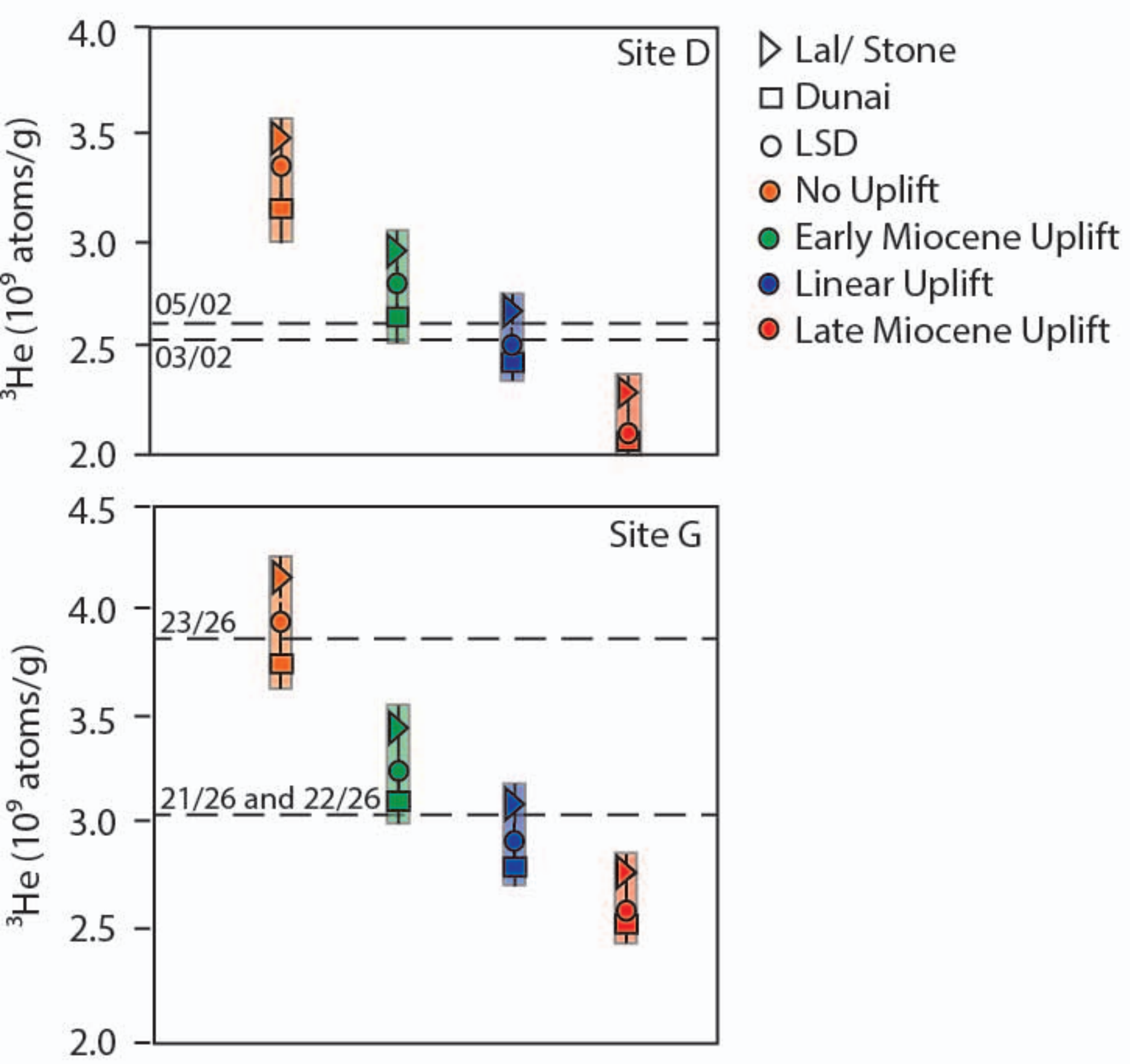
Site D
Site G
Lal/ Stone
Dunai
LSD
No Uplift
Early Miocene Uplift
Linear Uplift
Late Miocene Uplift
^{3}He (10^9 atoms/g)
4.0
3.5
3.0
2.5
2.0
05/02
03/02
4.5
23/26
21/26 and 22/26